

Published in final edited form as:

Circ Res. 2014 October 10; 115(9): 759–769. doi:10.1161/CIRCRESAHA.115.304164.

mir33 Inhibition Overcomes Deleterious Effects of Diabetes on Atherosclerosis Plaque Regression in Mice

Emilie Distel¹, Tessa J. Barrett¹, Kellie Chung¹, Natasha M. Girgis², Saj Parathath¹, Christine C. Essau³, Andrew J. Murphy^{4,5}, Kathryn J. Moore¹, and Edward A. Fisher¹

¹Leon H. Charney Division of Cardiology and Marc and Ruti Bell Program in Vascular Biology, Department of Medicine, New York University School of Medicine, New York, NY 10016, USA

²Department of Microbiology, New York University School of Medicine, New York, New York, NY 10016, USA

³Regulus Therapeutics, San Diego, California, USA

⁴Division of Molecular Medicine, Department of Medicine, Columbia University, New York, NY 10032, USA

⁵Haematopoiesis and Leukocyte Biology, Baker IDI Heart and Diabetes Institute, Melbourne, Australia

Abstract

Rationale—Diabetes increases cardiovascular disease risk in humans and remains elevated despite cholesterol-lowering therapy with statins. Consistent with this, in mouse models diabetes impairs atherosclerosis plaque regression after aggressive cholesterol-lowering. miR33 is a key negative regulator of the reverse cholesterol transport factors, ABCA1 and HDL, which suggested that its inhibition may overcome this impairment.

Objective—To assess the effects of miR33 inhibition on atherosclerosis regression in diabetic mice.

Methods and Results—Reversa mice, which are deficient in the LDL receptor and in which hypercholesterolemia is reversed by conditional inactivation of the microsomal triglyceride transfer protein (*Mttp*) gene, were placed on an atherogenic diet for 16 weeks, then either made diabetic by STZ injection or kept normoglycemic. Lipid-lowering was induced by *Mttp* inactivation and mice were treated with anti-miR33 or control oligonucleotides. Whereas regression was impaired in diabetic mice treated with control oligonucleotides, anti-miR33 treatment decreased plaque macrophage content and inflammatory gene expression in these mice.

Address correspondence to: Dr. Edward A. Fisher, New York University School of Medicine, 522 First Avenue, Smilow 701, New York, NY 10016, USA, Phone: 212.263.6631, Fax: 212.263.6632, edward.fisher@nyumc.org. Dr. Kathryn J. Moore, New York University School of Medicine, 522 First Avenue, Smilow 701, New York, NY 10016, USA, Phone: 212.263.6631, Fax: 212.263.6632, kathryn.moore@nyumc.org.
E.D. and T.J.B. contributed equally to this study.

DISCLOSURES

ED, TJB, KG, SP, AMJ: none

CCE: at the time of these studies, was a full-time employee at Regulus Therapeutics

KJM, EAF: Past members of Regulus Therapeutics Clinical Advisory Board

The decreased macrophage content in anti-miR33-treated diabetic mice was associated with a blunting of hyperglycemia-induced monocytosis and reduced monocyte recruitment to the plaque, which was traced to an inhibition of the proliferation of bone marrow monocyte precursors associated with the upregulation of their *Abca1*.

Conclusions—miR33 inhibition overcomes deleterious effects of diabetes in atherosclerosis regression in mice, which suggests a therapeutic strategy in diabetic patients, who remain at elevated cardiovascular disease risk despite plasma cholesterol lowering.

Keywords

Atherosclerosis; diabetes mellitus; regression; miR33; high-density lipoprotein; microRNA

INTRODUCTION

Diabetes increases the clinical risk of cardiovascular morbidity and mortality. This risk remains elevated with conventional LDL-cholesterol lowering therapies, such as statins¹. In the FIELD study, type 2 diabetic patients with mixed dyslipidemia (high triglycerides and low HDL-cholesterol (HDL-C)) showed the most benefit of combination fenofibrate/statin therapy, suggesting the importance of raising HDL-C in these patients². In mouse models, diabetes dramatically accelerates the progression of atherosclerosis³ and we have shown that it inhibits atherosclerosis regression following aggressive LDL reduction. This was due to increased monocyte infiltration and macrophage burden in the plaque compared to non-diabetic mice^{4, 5}. The plaque macrophages from diabetic mice also exhibited an M1 inflammatory phenotype, unlike the M2 inflammation-resolving/tissue remodeling macrophages we have typically found in regressing plaques in non-diabetic mice^{4, 6}. These impairments were largely driven by hyperglycemia, as glucose reduction improved the response to lipid lowering⁵. Notably, this restored regression was associated with reduced circulating monocyte levels as a result of the loss of the proliferative stimulus that hyperglycemia has on monocyte bone marrow progenitor cells⁵.

In non-diabetic atherosclerotic mice, increasing the plasma level of HDL by providing apoA1 (by transgenesis⁷ or infusion⁸) or by anti-miR33 treatment⁹ promotes plaque regression with an enrichment of macrophages expressing anti-inflammatory M2 markers. An important component of this beneficial effect of HDL is ascribed to its ability to promote cholesterol efflux from macrophages in the plaque. This process is mediated by the ABC transporters, ABCA1 and ABCG1, which provide cholesterol to lipid-poor and spherical HDL particles, respectively. In the liver, ABCA1 also provides phospholipids to newly secreted apoA1 to generate nascent lipid-poor HDL particles. We have previously shown that *Abca1* and *Abcg1* mRNAs are both targets of miR33¹⁰ and that treatment of *Ldlr*^{-/-} mice with anti-miR33 up-regulated ABCA1 in the liver and macrophages and resulted in plaque regression⁹. Taken with our findings that both *Abca1* and *Abcg1* are down-regulated by hyperglycemia¹¹, which may contribute to impaired regression of atherosclerosis in diabetic mice after plasma lipid lowering, this made anti-miR33 treatment an attractive candidate for overcoming this impairment.

To test this hypothesis, we turned to the Reversa mouse, which we have reported to be a model of atherosclerosis regression¹². To create a regression environment after plaques develop, the hyperlipidemia of the LDL receptor knockout (*Ldlr*^{-/-}) mouse is suppressed by the conditional inactivation of the microsomal triglyceride transfer protein gene (*Mttp*), which shuts down the secretion by the liver of VLDL (the precursor of LDL). As clinical studies show that atherosclerotic plaque formation starts before the onset of diabetes¹³, our protocol was to first establish atherosclerosis by placing mice on a western diet for 16 weeks, and then inducing diabetes with streptozotocin (STZ) in a subset of mice. We then tested the effects of anti-miR33 (or control oligonucleotides) in both normoglycemic and diabetic mice after plasma lipid normalization.

Consistent with our previous results⁴, regression was impaired by diabetes in control oligonucleotide treated mice, but inhibition of miR33 caused a significant decrease in the content and inflammatory state of plaque macrophages. These beneficial effects of anti-miR33 therapy were associated with changes in the population of circulating monocytes and their bone marrow precursors, as will be presented. Overall, the results suggest that targeting of miR33 may improve cardiovascular risk reduction by statins and other lipid-lowering therapies in patients with hyperglycemia.

METHODS

Animals

Reversa mice (*Ldlr*^{-/-}; ApoB^{100/100}; *Mtpp*^{fl/fl}; Mx1-Cre^{+/+})¹⁴ and C57Bl6J were cared for in accordance with the National Institutes of Health guidelines and the New York University Institutional Animal Care and Use Committee (Protocol 090908). Reversa pups were weaned at 4–5 weeks and placed on a western diet (21% (wt/wt) fat, 0.15% cholesterol (Research Dyets)) to allow the development of atherosclerotic plaques. After 15 weeks, mice were injected i.p. daily with STZ (50 mg/kg, Sigma-Aldrich) or citrate buffer for 5 days to induce diabetes or serve as a control. One week later, all mice were switched to a chow diet. Following the diet switch Reversa mice were injected i.p. with polyinosinic polycytidylic RNA (pIpC) (Sigma-Aldrich 15 mg/kg) every other day for a total of four injections⁴. Mice were then treated subcutaneously 4 times with the anti-sense oligonucleotides (ASO) anti-miR33 or the ASO control (Regulus Therapeutics, 10mg/kg) as previously described⁹. Regulus Therapeutics provided 2' fluoro/methoxyethyl (2'F/MOE) modified, phosphorothioate backbone modified anti-miR33 (TGCAATGCAACTACAATGCAC) and mismatch control (TCCAATCCAATTCATC) anti-miR. At sacrifice, mice were anesthetized with xylazine/ketamine and blood was collected via cardiac puncture for plasma analyses. Mice were perfused with PBS, followed by 10% sucrose in PBS. Aortic roots were embedded in OCT medium and frozen immediately, and tissues were snap-frozen under liquid nitrogen and stored at -80°C until further use.

Plasma lipoprotein analyses

Total cholesterol, HDL-cholesterol (HDL-C), and triglyceride (TG) concentrations were measured using colorimetric assays (all kits from Wako Diagnostics, Richmond, VA).

Glycemia was measured after 4 hours of fast with a blood glucometer (Freestyle lite, Roche).

Histochemical analyses

Aortic roots were harvested, frozen in OCT, and serial-sectioned at a thickness of 6 μm onto glass slides. For immunostaining of CD68 (macrophage marker), slides were fixed in 100% acetone and exposed to primary anti-CD68 antibody (Serotec), followed by biotinylated secondary antibody (Vector Laboratories), with visualization using a Vectastain ABC kit (Vector Laboratories). Microscopic images of aortic root sections were digitized, and morphometric measurements were performed using Image Pro Plus software (Micro Optical Solutions).

For collagen content, tissues were stained with picrosirius red and quantified with Image Pro Plus software using polarizing light microscopy.

Necrosis analysis

Necrosis, an indicator of the effectiveness of efferocytosis, was quantified in aortic roots from Reversa mice by measuring the acellular areas of plaques with Image Pro Plus software¹⁵.

Apoptosis analysis

Apoptosis was analyzed in aortic roots from Reversa mice by TUNEL method using an *in situ* cell detection kit (Roche Diagnostics). Nuclei were labeled with Vectashield Mounting media with DAPI (Vector labs). Only TUNEL positive cells that colocalized with DAPI-stained nuclei were considered apoptotic.

Laser capture microdissection

CD68⁺ cells were isolated from atherosclerotic plaques by laser capture micro-dissection (LCM)^{16, 17}. All LCM procedures were performed under RNase-free conditions. Aortic root sections were stained with hematoxylin-eosin and captured from 36 frozen sections. After LCM, RNA was isolated using the PicoPure Kit (Molecular Devices), and quality and quantity were determined using an Agilent 2100 Bioanalyzer (Agilent Technologies). RNA was converted to cDNA and amplified using the WT-Ovation Pico RNA Amplification Kit (NuGEN). Real-time PCR was performed with 5ng of amplified cDNA using the ABI PRISM 7300 sequence detection system (Applied Biosystems). Gene expression was assessed using the Ct calculation method.

Monocyte tracking

Monocytes were labeled as previously described^{18, 19}. Briefly, 1 μm Fluoresbrite FITC-dyed (YG) plain microspheres (Polysciences Inc.) were diluted in PBS (1:4), and 250 μl of the solution was injected into the retro-orbital vein of mice to label circulating Ly6C^{lo} monocytes. For the egress study, beads were injected at week 14 before any treatment. For the recruitment study, beads were injected 24h prior to harvesting. For both protocols, bead labeling efficiency was assessed by flow cytometry, 24h after bead injection^{18, 19}.

Flow cytometry

Blood Leukocytes—Blood was collected *via* retro orbital bleeding with EDTA-coated capillaries. Red blood cells were lysed with RBL buffer (Sigma Aldrich), and blocking achieved with anti-mouse CD16/CD32 (eBioscience). Monocytes were identified by staining with PE anti-mouse CD115 (Biolegend) and APC anti-mouse Ly-6G/Ly-6C (Biolegend)^{18, 19}. Neutrophils were identified as CD45^{hi}CD115^{lo}Ly6-C/G^{hi} cells. Flow cytometry was performed using a LSRII analyzer.

Hematopoietic stem and progenitor cells—Hematopoietic stem and progenitor cells were analyzed by flow cytometry as previously described^{5, 20}. Briefly, bone marrow was harvested from femurs and tibias, and red blood cells were lysed with BD Pharm Lyse (BD Biosciences). Cells were incubated with a cocktail of antibodies against lineage-committed (lin) cells (B220, CD19, CD11b, CD3e, TER-119, CD2, CD8, CD4, Ly6-C/Ly6-G, all FITC) and markers to identify the stem and progenitor cells that were identified as LSK (lin⁻, Sca1⁺, and ckit⁺), CMP (lin⁻, Sca1⁻, ckit⁺, CD34^{int}, and FcγRII^{int}/FcγRIII^{int}), and GMP (lin⁻, Sca1⁻, ckit⁺, CD34^{int}, and FcγRII^{hi}/FcγRIII^{hi}). Cell cycle analysis was performed using DAPI (Sigma Aldrich) to measure cells in the S-G₂M phase, G₀ and sub-G₀ (apoptotic). Flow cytometry was performed using an LSR II (for analysis) or MoFlo (for sorting). All flow cytometry data were analyzed using FlowJo X software (Tree Star). RNA from sorted cells was extracted with RNeasy Micro kit (Qiagen) and cDNA was obtained with SuperScript VILO (Life Technologies).

Statistical analysis

For atherosclerosis and immunohistochemical analyses, all comparisons were made using a 1-way ANOVA (P 0.05), and data are expressed as mean ± SEM.

RESULTS

Anti-miR33 increases HDL-C and target gene expression in livers of diabetic mice

To assess the effects of miR33 inhibition on atherosclerosis regression in a hyperglycemic environment, Reversa mice were fed a western diet (WD; 21% fat, 0.15% cholesterol) for 16 weeks to allow complex plaques to develop (see Figure 1A for a schematic depiction of the overall protocol). At 15 weeks, mice were given daily (i.p.) injections for 5 consecutive days with citrate buffer or 50 mg/kg streptozotocin (STZ) to induce diabetes⁴. At 16 weeks, all mice were switched to a standard chow diet (6% fat) and injected i.p. four times every other day with pIpC to conditionally delete the *Mtpp* gene and induce lipid lowering. *Mtpp* deletion resulted in effective cholesterol lowering compared to baseline levels (baseline: 863±47 mg/dL to 83–101 mg/dL in the experimental groups; Table 1). The reduction in total cholesterol levels was independent of STZ or anti-miR (control or miR33) treatment.

Following pIpC injections, mice were treated weekly by subcutaneous injection with either miR33 or control ASOs. After 4 weeks, anti-miR33 treatment increased HDL-C by 30% (p 0.05) and 42% (p 0.05) in the normoglycemic and in the diabetic groups, respectively (Table 1). Anti-miR33 treatment did not affect the blood glucose levels of either the normoglycemic or diabetic mice when compared to the corresponding ASO control-treated

mice (Table 1). Consistent with previous observations in mouse models²¹ and diabetic patients²², plasma triglyceride levels were increased by hyperglycemia; no effect of anti-miR33 on triglyceride levels was observed when compared to control ASO treated mice (Table 1).

The efficacy of miR33 inhibition was evaluated by measuring the expression of known target mRNAs in the liver. As previously reported¹⁰, anti-miR33 treatment significantly increased *Abca1* mRNA expression (p 0.05) in normoglycemic mice (Figure 1B). Furthermore, although *Abca1* mRNA was reduced by almost 50% (p 0.05) in the livers of hyperglycemic mice, anti-miR33 treatment restored *Abca1* expression to the level seen in normoglycemic anti-miR33 treated mice (Figure 1B). *Abcg1* expression in the livers of diabetic mice was modestly reduced compared to normoglycemic mice (Figure 1C). Anti-miR33 treatment increased *Abcg1* mRNA levels by 1.5-fold (p 0.05) in the diabetic mice, whereas no effect of anti-miR33 was observed in normoglycemic mice. Levels of *Cpt1* mRNA, another miR33 target gene, were also increased by anti-miR33 treatment in both normo- and hyperglycemic mice (p 0.05; Figure 1D). Non-miR33 target genes, such as HMG-CoA reductase, were not affected by anti-miR33 treatment (Figure 1E), although its expression was increased in the diabetic mice (p 0.05; Figure 1E), as previously reported²³.

Anti-miR33 reduces plaque macrophage content in diabetic mice after plasma lipid lowering

Anti-miR33 treatment has been shown to promote plaque regression in *Ldlr*^{-/-} mice fed WD for 16 weeks, and then switched to chow for the duration of treatment (4 weeks). This beneficial effect of anti-miR33 was associated with increased HDL-C and reverse cholesterol transport, presumably as a consequence of greater *Abca1* expression in liver and plaque macrophages⁹. Consistent with our previous findings⁴, we observed that diabetes impaired plaque regression after lowering of plasma cholesterol as reflected by the decrease in plaque macrophage content (CD68⁺ cells) in the normoglycemic group (p 0.001), but not in the diabetic group (Figure 2). Anti-miR33 treatment restored plaque regression in the diabetic group, and reduced macrophage content to the same level observed in normoglycemic mice. Interestingly, anti-miR33 treatment did not further reduce plaque macrophage content in the non-diabetic group, suggesting that in the absence of hyperglycemia, the reduction in plasma cholesterol level alone was sufficient to drive this process, as shown by the ~50% decrease of plaque CD68 content compared to baseline (Figure 2; Baseline 52% vs. Regression + anti-miR33 26±2.2%, p 0.05). As we have observed previously⁴, reduction in macrophage content did not result in changes in total plaque area (Online Figure I), which has been shown to be from increases in plaque collagen content in the regressing plaque. Consistent with this, anti-miR33 treatment increased the plaque collagen content in the diabetic group, restoring it to the same level observed in normoglycemic mice (Figure 2B). Together, these data suggest that anti-miR33 treatment promotes a remodeling of the diabetic plaque towards a more stable-appearing phenotype.

Anti-miR33 treatment favorably alters plaque macrophage inflammatory phenotype in diabetic mice after plasma lipid lowering

We next assessed the effects of anti-miR33 on the phenotype of diabetic plaque macrophages by analyzing mRNA expression of laser-captured cells. Consistent with our previous findings^{4, 5}, macrophages in the plaques from control anti-miR treated diabetic mice showed a pattern of gene expression predominantly of the inflammatory M1 phenotype (e.g. increased *Il1 β* , *Tnfa*) and also had reduced expression of *Abca1* (Table 2). Notably, anti-miR33 treatment of diabetic mice reduced mRNAs of M1 macrophage-related genes (*Il1 β* , *Tnfa*, *Nos2*) and increased those of anti-inflammatory M2 macrophage-related genes (*Ym1*, *Cd206*). Furthermore, treatment with anti-miR33 restored levels of macrophage *Abca1* mRNA in the diabetic group to that observed in normoglycemic mice (Table 2). These findings suggest that anti-miR33 treatment dampened the persistent inflammation in the plaque associated with hyperglycemia.

Anti-miR33 treatment reduces plaque monocyte recruitment, but does not change macrophage egress

A decrease in macrophage content in the regressing plaque could be due to reduced recruitment of monocytes to the plaque, loss of macrophages through egress (regulated by retention and chemotaxis), or macrophage death⁶. To investigate the mechanisms underlying the reduction in macrophages in diabetic plaques by anti-miR33 treatment, we used an *in vivo* bead-labeling technique^{12, 19} to assess monocyte recruitment and macrophage egress. To measure the recruitment of monocytes, mice were injected with fluorescent latex beads 24h before the harvesting of aortic roots and the number of beads in the plaques counted. Monocyte labeling was not affected by either diabetes or anti-miR treatment, indicating that neither condition had a significant effect on the phagocytic ability of circulating monocytes (Online Figure II). Hyperglycemia was associated with a 60% increase in monocyte recruitment to the plaque (p 0.01; Figure 3B), consistent with our previous observations in another model of regression⁵. Notably, anti-miR33 treatment prevented this diabetes-induced increased recruitment of monocytes (p 0.01; Figure 3B). Although these results could be attributed in large part to changes in the circulating number of monocytes (see below), studies *in vitro* suggested that anti-miR33 treatment could also have caused an intrinsic decrease in monocyte/macrophage chemotaxis in a hyperglycemic environment (Online Figure IIIA & IIIB).

To study macrophage egress, we injected fluorescent beads prior to the induction of diabetes or anti-miR treatment (week 14, Figure 3A). One week after bead injection, a group of mice was sacrificed to obtain baseline measurements of the content of labeled macrophages (i.e. CD68⁺ cells co-localized with beads) in aortic root plaques. As in the experiment described above, additional mice were then treated with STZ, pIpC and anti-miR (control or miR33, Figure 3A), and the beads remaining in the aortic root plaques at sacrifice were quantified. Reversal of hyperlipidemia was associated with a reduction in plaque bead content to ~50% of baseline independent of the treatment (p 0.001; Figure 3C). These results suggest that though macrophages were actively leaving the plaque during regression, this process was not differentially affected by diabetes or anti-miR33 treatment. Consistent with this was the

lack of significant changes in the plaque macrophage expression of the chemotactic factor *Ccr7*²⁴ or of the retention factor²⁴ *Netrin-1* and its receptor, *Unc5b*²⁵ (Table 2).

Anti-miR33 treatment does not affect plaque macrophage apoptosis, but does increase efferocytosis

Plaque macrophage content can also be modulated by apoptosis, but we did not observe any significant differences in this among the groups as measured by TUNEL analysis (Figure 3D). Diabetes, however, promoted an increase in the area occupied by necrotic cores, which negatively reflects the level of efferocytotic activity¹⁵, compared to plaques from regressing normoglycemic mice (Figure 3E, $p < 0.05$), similar to its effects in progression²⁶. Notably, anti-miR33 treatment of diabetic mice significantly reduced the plaque necrotic area to that of normoglycemic mice (Figure 3E, $p < 0.05$), suggesting that diabetes-associated deficiencies in efferocytosis were corrected.

Anti-miR33 treatment reduces hyperglycemia-induced monocytosis, but not neutrophilia

The increased recruitment of monocytes in the diabetic mice after plasma lipid reduction may be a consequence of the higher numbers of circulating monocytes observed in mice that have hyperglycemia, which are also elevated with hypercholesterolemia^{18–20}. Indeed, in the present study, plasma lipid lowering induced a significant decrease in the level of monocytes (expressed as their % of circulating leukocytes) compared to baseline ($p < 0.001$; Figure 4A, B). Lipid lowering, however, had no effect on the monocyte levels in the control anti-miR treated diabetic group, likely due to the increased monocyte precursor proliferation *via* glucose-dependent mechanisms⁵. In contrast, anti-miR33 treatment decreased monocyte levels in the diabetic mice to levels comparable to the non-diabetic mice ($p < 0.001$; Figure 4A, B).

In addition to the monocytosis, hyperglycemia induced neutrophilia, as we previously observed⁵, but this was not affected by cholesterol lowering in the regression period or by anti-miR33 treatment (Figure 4C).

Anti-miR33 treatment reduces bone marrow monocyte progenitors in diabetic mice

We previously showed that diabetes induces myelopoiesis in the bone marrow (BM)⁵, and it has also been shown that the membrane content of cholesterol, as influenced by cholesterol efflux-related genes and plasma cholesterol levels, positively regulates myeloid cell production by increasing BM progenitor cell proliferation^{20, 27, 28}. Because the anti-miR33 treatment is given concurrent with plasma lipid lowering, to study the effects of anti-miR33 on BM progenitors, we used normolipidemic C57Bl/6J (WT) mice, to avoid the confounding effects of hypercholesterolemia²⁰.

A group of mice were made diabetic with STZ and treated with control anti-miR or anti-miR33 weekly for 4 weeks as before. Treatment with the control anti-miR or anti-miR33 had no effect on blood glucose levels (Figure 5A) or on plasma levels of total cholesterol and triglycerides (Online Figure IVA and IVB). As expected, anti-miR33 significantly increased HDL-C in both diabetic and normoglycemic mice (Figure 5B, Online Figure IVB). Consistent with our previous findings⁵, hyperglycemia induced an increase in the

abundance and proliferation of both common myeloid (CMP) and granulocyte-macrophage progenitor cells (GMP), without affecting the stem cells (LSK) (Figure 5C & D). This was accompanied by a reduction of CMP and GMP, but not LSK in the G0 phase, confirming entry into the proliferative cell cycle (Online Figure VA). Importantly, the reduction in the abundance and proliferation of myeloid precursors with anti-miR33 in the diabetic mice was not due to enhanced apoptosis (Online Figure VB) or senescence (Online Figure VC).

Treatment with anti-miR33 reduced the expansion and proliferation of the CMP and GMP in the diabetic mice (Figure 5C, 6D), indicating that anti-miR33 acts *via* glucose-independent mechanisms to inhibit the production of monocytes in diabetes. This effect of anti-miR33 treatment on proliferation of monocyte progenitors, however, was not observed in macrophages *in vitro*; while there was evidence of their increased proliferation in a hyperglycemic environment, it was not suppressed by anti-miR33 treatment (Online Figure IIC).

Anti-miR33 treatment restores ABCA1 and ABCG1 gene expression in bone marrow monocyte progenitor cells

ABCA1 and ABCG1 have been shown to play a crucial role in hematopoietic stem cell proliferation^{28, 29}. We hypothesized that hyperglycemia-induced BM progenitor proliferation was due to a defect of *Abca1/Abcg1* expression in the different progenitor subsets, which would increase the plasma membrane cholesterol content of these cells, stimulating their proliferation²⁸. Indeed, as observed in the liver and in plaque macrophages, *Abca1* and *Abcg1* gene expression was decreased by hyperglycemia in the CMP (Figure 6B) and GMP (Figure 6C), without affecting expression in the LSK population (Figure 6A). Notably, anti-miR33 treatment restored *Abca1* expression in both the CMP and GMP subset (Figure 6B, 6C). These results suggest that anti-miR33 may prevent monocytois at the level of BM progenitor cells, through its upregulation of *Abca1* expression in those cells.

DISCUSSION

Diabetic patients after cholesterol lowering remain at higher risk of CVD relative to non-diabetics. Consistent with this, is our finding in two independent mouse models that after cholesterol-lowering, atherosclerosis regression is impaired by hyperglycemia^{4, 5}. Because anti-miR33 treatment regressed plaques in non-diabetic mice⁹, we reasoned that a similar approach may overcome this impairment. Indeed, our results show that miR33 inhibition confers a number of atheroprotective benefits in the context of hyperglycemia, chief among them being the reduction in the content and inflammatory state of plaque macrophages. This was found to be due to the ability of anti-miR33 to reduce the monocytois associated with diabetes, which decreased the continued recruitment of monocytes into plaques that occurs even in the face of lipid lowering³⁰. These findings, then, expand the atheroprotective mechanisms of anti-miR33 to the diabetic setting, an area of great clinical importance.

Although we observed, as before¹², egress of macrophages after plasma lipid lowering in *Reversa* mice, this was not further increased by anti-miR33 treatment in either normo- or hyperglycemic mice. The lack of increase in egress associated with anti-miR33 treatment was consistent with the absence of changes in the gene expression of previously identified

factors affecting this pathway, including the chemotactic factor *Ccr7* or the retention factor *Netrin-1*. We also observed no changes in plaque macrophage apoptosis and senescence or in macrophage proliferation *in vitro* with anti-miR33 treatment, but did find evidence for increased efferocytosis, as judged by necrotic core analysis. Thus, the basis for the reduction in plaque macrophage content in the diabetic mice by anti-miR33 appears to derive primarily from decreased recruitment of monocytes into the plaques and increased clearance of apoptotic cells. That recruitment continues in a regression environment has been previously established^{18, 30}, and the present results represent another demonstration that its reduction can contribute to decreased plaque content of macrophages after cholesterol lowering^{5,18}.

As we recently reported in another mouse model, hyperglycemia induces monocytosis due to BM progenitor proliferation, and this in turn results in increased recruitment of these cells to plaques after reduction in the plasma lipid level⁵. As shown in Figure 4 and 6, anti-miR33 treatment reduced monocytosis and BM progenitor proliferation despite persistence of the hyperglycemia, thereby preventing the expansion of the pool of recruitable cells by hyperglycemia. These findings are related to the report from Yvan-Charvet et al.²⁸ that links cholesterol efflux-related genes in the BM progenitors to their proliferation and subsequent production of monocytes. Yvan-Charvet and colleagues showed that deficiency of *Abca1* and *Abcg1*, even in the non-hyperlipidemic setting, led to monocytosis and leukocyte infiltration into tissues, presumably through changes in plasma membrane cholesterol that affected responsiveness to proliferative factors.²⁸ In the present study, hyperglycemia induced a decrease in *Abca1* and *Abcg1* expression in the BM progenitors (Figure 6), which would be expected to be a proliferative stimulus. Restoration of *Abca1* and *Abcg1* expression with anti-miR33 treatment, therefore, would be predicted to normalize BM proliferation and the level of circulating monocytes, just as observed. Because monocytosis is also observed in people with diabetes and correlates with their risk of cardiovascular disease³¹, it is tempting to speculate that anti-miR33 therapy would be effective in that population to reduce this risk, in part, through similar effects in human bone marrow.

We previously reported that when plasma lipids are lowered, in addition to the reduction in the plaque content of macrophages, the inflammatory state of these cells is also lowered in normoglycemic, but not hyperglycemic, mice^{4, 7, 12}. As also previously reported⁹, anti-miR33 treatment induces an enrichment in “anti-inflammatory” M2 macrophages. In the present study, consistent with this, and shown in Table 2, miR33 inhibition reversed this adverse effect of hyperglycemia on plaque macrophage inflammation. There are at least two potential bases for this. One could be related to previous findings from the laboratories of Alan Tall³² and John Parks³³ that showed that free cholesterol enrichment of the plasma membrane, particularly in lipid-rafts in macrophages with ABCA1-deficiency, leads to enhanced inflammatory signaling *via* Toll-like receptors (TLRs). That the down-regulation of *Abca1* by hyperglycemia and the restoration of its expression by anti-miR33 modulated plaque macrophage inflammatory state through this mechanism is supported by finding that increases in *Ccr2*, *Vcam1* and *Icam1*, all NF-κB targets downstream of TLR-signaling, were reversed by anti-miR33. Despite *Abcg1* also being a NF-κB target^{34,9}, its gene expression was not changed in plaque macrophages or in CMP precursors, suggesting that under our

experimental conditions, ABCG1 may be more likely in these cell types to be regulated by post-transcriptional mechanisms.

The other potential basis, particularly for the enrichment in M2 features, is that direct or indirect targets that promote the M2 phenotypic state of macrophages were de-repressed by the anti-miR33 treatment. A previous report³⁵ has also implicated the eicosanoid pathway in the inflammatory process of diabetes-accelerated atherosclerosis. In the present studies, however, we found no significant evidence to suggest this pathway as a mechanism for the effects of anti-miR33 treatment, as judged by the lack of change in the gene expression of the major related enzymes (*Acs11*, *Pges1*, *Ptges*; data not shown).

It is interesting to compare the benefits of anti-miR33 treatment in atherosclerosis regression to those in progression. Recent studies report conflicting results. Rotllan et al.³⁶ and Horie et al.³⁷ showed that miR33 inhibition, either by therapeutic or by genetic silencing, lead to a delay in plaque progression. Marquart et al.³⁸, however, did not observe any differences in atherosclerosis progression between anti-miR33 treated and control oligonucleotide-treated mice. The major differences between the studies were the oligonucleotide inhibitors of miR33 used and the amount of cholesterol in the diets (0.15%³⁷, 0.3%³⁶ vs. 1.25%³⁸), which resulted in a wide range of plasma cholesterol levels. It appears that when plasma cholesterol was above 1200 mg/dL, anti-miR33 was less able to be atheroprotective.

A qualitatively similar phenomenon may also occur in regression. We have seen in another mouse model of atherosclerosis that anti-miR33 treatment was able to improve the content and inflammatory state of the macrophages in the normoglycemic setting, but in that study, the plasma cholesterol levels were 250 mg/dL in the treatment groups⁹, compared to <100 mg/dL in the present study. The lack of an effect on regression of miR33 inhibition in the normoglycemic group in the present study, then, likely reflects that the plasma cholesterol level was sufficiently low so that no further treatment benefit would be realized unless there was the concurrent stress of hyperglycemia. Thus, like many therapeutics tested for cardiovascular disease risk reduction, there is likely a range of plasma cholesterol levels above which the effects of anti-miR33 treatment are attenuated and below which it cannot exert further improvements, with the range potentially dependent on the presence of co-morbidities.

In conclusion, the present results show for the first time that miR33 inhibition is able to overcome the deleterious effects of hyperglycemia on plaque regression in atherosclerotic mice after their plasma lipids were aggressively lowered. Because we did not test the effects of miR33 inhibition in a setting of hyperglycemia *and* insulin resistance, the full relevance of our findings to patients with type 2 diabetes mellitus remains to be established. Nevertheless, given that patients with either type 1 and 2 diabetes mellitus both have hyperglycemia and high rates of cardiovascular disease, it is tempting to suggest that anti-miR33 treatment as a promising combination strategy to make statins and other lipid-lowering therapies more effective in these patients to reduce their elevated risk.

Supplementary Material

Refer to Web version on PubMed Central for supplementary material.

Acknowledgments

SOURCES OF FUNDING

NIH funding: KJM: R01 HL108182; EAF: R01 DK095684, R01 HL117226, R01 HL084312, P01 HL098055. AJM was supported by post-doctoral fellowship 12POST11890019 from the American Heart Association and a Viertel award from Diabetes Australia Research Trust.

Nonstandard Abbreviations and Acronyms

ABCA1	ATP-binding cassette transporter A1
ABCG1	ATP-binding cassette transporter G1
ASO	Anti-sense oligonucleotides
BM	Bone marrow
CMP	Common myeloid progenitor
GMP	Granulocyte-macrophage progenitor
LSK	Lin ⁻ , Sac1 ⁺ , ckit ⁺ stem cells
LCM	Laser capture micro-dissection
miR33	microRNA 33
Mttp	Microsomal triglyceride transfer protein
pIpC	Polyinosinic polycytidylic
STZ	Streptozotocin

References

1. Beckman JA, Creager MA, Libby P. Diabetes and atherosclerosis: epidemiology, pathophysiology, and management. *JAMA*. May 15.2002 287:2570–2581. [PubMed: 12020339]
2. Sacks FM. After the Fenofibrate Intervention and Event Lowering in Diabetes (FIELD) study: implications for fenofibrate. *Am J Cardiol*. Dec 22.2008 102:34L–40L.
3. Vikramadithyan RK, Hu Y, Noh HL, Liang CP, Hallam K, Tall AR, Ramasamy R, Goldberg IJ. Human aldose reductase expression accelerates diabetic atherosclerosis in transgenic mice. *J Clin Invest*. Sep.2005 115:2434–2443. [PubMed: 16127462]
4. Parathath S, Grauer L, Huang LS, Sanson M, Distel E, Goldberg IJ, Fisher EA. Diabetes adversely affects macrophages during atherosclerotic plaque regression in mice. *Diabetes*. Jun.2011 60:1759–1769. [PubMed: 21562077]
5. Nagareddy PR, Murphy AJ, Stirzaker RA, Hu Y, Yu S, Miller RG, Ramkhelawon B, Distel E, Westertep M, Huang LS, Schmidt AM, Orchard TJ, Fisher EA, Tall AR, Goldberg IJ. Hyperglycemia promotes myelopoiesis and impairs the resolution of atherosclerosis. *Cell Metab*. May 7.2013 17:695–708. [PubMed: 23663738]
6. Moore KJ, Sheedy FJ, Fisher EA. Macrophages in atherosclerosis: a dynamic balance. *Nat Rev Immunol*. Oct.2013 13:709–721. [PubMed: 23995626]
7. Feig JE, Rong JX, Shamir R, Sanson M, Vengrenyuk Y, Liu J, Rayner K, Moore K, Garabedian M, Fisher EA. HDL promotes rapid atherosclerosis regression in mice and alters inflammatory

- properties of plaque monocyte-derived cells. *Proc Natl Acad Sci U S A*. Apr 26.2011 108:7166–7171. [PubMed: 21482781]
8. Hewing B, Parathath S, Barrett T, Chung WKK, Astudillo YM, Yamada T, Ramkhalawon B, Tallant TC, Yusufishaq MSS, DiDonato JA, Yuang Y, Berisha SZ, Hazen SL, Smith JD, Fisher EA. Effects of native and myeloperoxidase-modified apolipoprotein a-I on reverse cholesterol transport and atherosclerosis in mice. *Arterioscler Thromb Vasc Biol*. 2014; 34:779–89. [PubMed: 24407029]
 9. Rayner KJ, Sheedy FJ, Esau CC, Hussain FN, Temel RE, Parathath S, van Gils JM, Rayner AJ, Chang AN, Suarez Y, Fernandez-Hernando C, Fisher EA, Moore KJ. Antagonism of miR-33 in mice promotes reverse cholesterol transport and regression of atherosclerosis. *J Clin Invest*. Jul. 2011 121:2921–2931. [PubMed: 21646721]
 10. Rayner KJ, Suarez Y, Davalos A, Parathath S, Fitzgerald ML, Tamehiro N, Fisher EA, Moore KJ, Fernandez-Hernando C. MiR-33 contributes to the regulation of cholesterol homeostasis. *Science*. Jun 18.2010 328:1570–1573. [PubMed: 20466885]
 11. Passarelli M, Tang C, McDonald TO, O'Brien KD, Gerrity RG, Heinecke JW, Oram JF. Advanced glycation end product precursors impair ABCA1-dependent cholesterol removal from cells. *Diabetes*. Jul.2005 54:2198–2205. [PubMed: 15983222]
 12. Feig JE, Parathath S, Rong JX, Mick SL, Vengrenyuk Y, Grauer L, Young SG, Fisher EA. Reversal of hyperlipidemia with a genetic switch favorably affects the content and inflammatory state of macrophages in atherosclerotic plaques. *Circulation*. Mar 8.2011 123:989–998. [PubMed: 21339485]
 13. Haffner SM, Lehto S, Ronnema T, Pyorala K, Laakso M. Mortality from coronary heart disease in subjects with type 2 diabetes and in nondiabetic subjects with and without prior myocardial infarction. *The New England journal of medicine*. Jul 23.1998 339:229–234. [PubMed: 9673301]
 14. Lieu HD, Withycombe SK, Walker Q, Rong JX, Walzem RL, Wong JS, Hamilton RL, Fisher EA, Young SG. Eliminating atherogenesis in mice by switching off hepatic lipoprotein secretion. *Circulation*. Mar 11.2003 107:1315–1321. [PubMed: 12628954]
 15. Thorp E, Tabas I. Mechanisms and consequences of efferocytosis in advanced atherosclerosis. *Journal of leukocyte biology*. Nov.2009 86:1089–1095. [PubMed: 19414539]
 16. Trogan E, Choudhury RP, Dansky HM, Rong JX, Breslow JL, Fisher EA. Laser capture microdissection analysis of gene expression in macrophages from atherosclerotic lesions of apolipoprotein E-deficient mice. *Proc Natl Acad Sci U S A*. Feb 19.2002 99:2234–2239. [PubMed: 11842210]
 17. Trogan E, Fisher EA. Laser capture microdissection for analysis of macrophage gene expression from atherosclerotic lesions. *Methods Mol Biol*. 2005; 293:221–231. [PubMed: 16028422]
 18. Potteaux S, Gautier EL, Hutchison SB, van Rooijen N, Rader DJ, Thomas MJ, Sorci-Thomas MG, Randolph GJ. Suppressed monocyte recruitment drives macrophage removal from atherosclerotic plaques of ApoE^{-/-} mice during disease regression. *J Clin Invest*. May.2011 121:2025–2036. [PubMed: 21505265]
 19. Tacke F, Alvarez D, Kaplan TJ, Jakubzick C, Spanbroek R, Llodra J, Garin A, Liu J, Mack M, van Rooijen N, Lira SA, Habenicht AJ, Randolph GJ. Monocyte subsets differentially employ CCR2, CCR5, and CX3CR1 to accumulate within atherosclerotic plaques. *J Clin Invest*. Jan.2007 117:185–194. [PubMed: 17200718]
 20. Murphy AJ, Akhtari M, Tolani S, Pagler T, Bijl N, Kuo CL, Wang M, Sanson M, Abramowicz S, Welch C, Bochem AE, Kuivenhoven JA, Yvan-Charvet L, Tall AR. ApoE regulates hematopoietic stem cell proliferation, monocytoysis, and monocyte accumulation in atherosclerotic lesions in mice. *J Clin Invest*. Oct.2011 121:4138–4149. [PubMed: 21968112]
 21. Kako Y, Huang LS, Yang J, Katopodis T, Ramakrishnan R, Goldberg IJ. Streptozotocin-induced diabetes in human apolipoprotein B transgenic mice. Effects on lipoproteins and atherosclerosis. *Journal of lipid research*. Dec.1999 40:2185–2194. [PubMed: 10588944]
 22. Ginsberg HN. Diabetic dyslipidemia: basic mechanisms underlying the common hypertriglyceridemia and low HDL cholesterol levels. *Diabetes*. Jul; 1996 45(Suppl 3):S27–30. [PubMed: 8674885]

23. Lally S, Owens D, Tomkin GH. Genes that affect cholesterol synthesis, cholesterol absorption, and chylomicron assembly: the relationship between the liver and intestine in control and streptozotocin diabetic rats. *Metabolism*. Mar.2007 56:430–438. [PubMed: 17292734]
24. Trogan E, Feig JE, Dogan S, Rothblat GH, Angeli V, Tacke F, Randolph GJ, Fisher EA. Gene expression changes in foam cells and the role of chemokine receptor CCR7 during atherosclerosis regression in ApoE-deficient mice. *Proc Natl Acad Sci U S A*. Mar 7.2006 103:3781–3786. [PubMed: 16537455]
25. van Gils JM, Derby MC, Fernandes LR, Ramkhalawon B, Ray TD, Rayner KJ, Parathath S, Distel E, Feig JL, Alvarez-Leite JI, Rayner AJ, McDonald TO, O'Brien KD, Stuart LM, Fisher EA, Lacy-Hulbert A, Moore KJ. The neuroimmune guidance cue netrin-1 promotes atherosclerosis by inhibiting the emigration of macrophages from plaques. *Nat Immunol*. Feb.2012 13:136–143. [PubMed: 22231519]
26. Bornfeldt KE, Tabas I. Insulin resistance, hyperglycemia, and atherosclerosis. *Cell Metab*. Nov 2.14:575–585. [PubMed: 22055501]
27. Tolani S, Pagler TA, Murphy AJ, Bochem AE, Abramowicz S, Welch C, Nagareddy PR, Holleran S, Hovingh GK, Kuivenhoven JA, Tall AR. Hypercholesterolemia and reduced HDL-C promote hematopoietic stem cell proliferation and monocytosis: studies in mice and FH children. *Atherosclerosis*. Jul.2013 229:79–85. [PubMed: 23684512]
28. Yvan-Charvet L, Pagler T, Gautier EL, Avagyan S, Siry RL, Han S, Welch CL, Wang N, Randolph GJ, Snoeck HW, Tall AR. ATP-binding cassette transporters and HDL suppress hematopoietic stem cell proliferation. *Science*. Jun 25.2010 328:1689–1693. [PubMed: 20488992]
29. van Eck M, Bos IS, Kaminski WE, Orso E, Rothe G, Twisk J, Bottcher A, Van Amersfoort ES, Christiansen-Weber TA, Fung-Leung WP, Van Berkel TJ, Schmitz G. Leukocyte ABCA1 controls susceptibility to atherosclerosis and macrophage recruitment into tissues. *Proc Natl Acad Sci U S A*. Apr 30.2002 99:6298–6303. [PubMed: 11972062]
30. Llodra J, Angeli V, Liu J, Trogan E, Fisher EA, Randolph GJ. Emigration of monocyte-derived cells from atherosclerotic lesions characterizes regressive, but not progressive, plaques. *Proc Natl Acad Sci U S A*. Aug 10.2004 101:11779–11784. [PubMed: 15280540]
31. Ford ES. Leukocyte count, erythrocyte sedimentation rate, and diabetes incidence in a national sample of US adults. *American journal of epidemiology*. Jan 1.2002 155:57–64. [PubMed: 11772785]
32. Sun Y, Ishibashi M, Seimon T, Lee M, Sharma SM, Fitzgerald KA, Samokhin AO, Wang Y, Sayers S, Aikawa M, Jerome WG, Ostrowski MC, Bromme D, Libby P, Tabas IA, Welch CL, Tall AR. Free cholesterol accumulation in macrophage membranes activates Toll-like receptors and p38 mitogen-activated protein kinase and induces cathepsin K. *Circulation research*. Feb 27.2009 104:455–465. [PubMed: 19122179]
33. Zhu X, Owen JS, Wilson MD, Li H, Griffiths GL, Thomas MJ, Hiltbold EM, Fessler MB, Parks JS. Macrophage ABCA1 reduces MyD88-dependent Toll-like receptor trafficking to lipid rafts by reduction of lipid raft cholesterol. *Journal of lipid research*. Nov.2010 51:3196–3206. [PubMed: 20650929]
34. Yvan-Charvet L, Kling J, Pagler T, Li H, Hubbard B, Fisher T, Sparrow CP, Taggart AK, Tall AR. Cholesterol efflux potential and antiinflammatory properties of high-density lipoprotein after treatment with niacin or anacetrapib. *Arterioscler Thromb Vasc Biol*. Jul.2010 30:1430–1438. [PubMed: 20448206]
35. Kanter JE, Kramer F, Barnhart S, Averill MM, Vivekanandan-Giri A, Vickery T, Li LO, Becker L, Yuan W, Chait A, Braun KR, Potter-Perigo S, Sanda S, Wight TN, Pennathur S, Serhan CN, Heinecke JW, Coleman RA, Bornfeldt KE. Diabetes promotes an inflammatory macrophage phenotype and atherosclerosis through acyl-CoA synthetase 1. *Proc Natl Acad Sci U S A*. Mar 20.109:E715–724. [PubMed: 22308341]
36. Rotllan N, Ramirez CM, Aryal B, Esau CC, Fernandez-Hernando C. Therapeutic silencing of microRNA-33 inhibits the progression of atherosclerosis in Ldlr^{-/-} mice—brief report. *Arterioscler Thromb Vasc Biol*. Aug.2013 33:1973–1977. [PubMed: 23702658]
37. Horie T, Baba O, Kuwabara Y, Chujo Y, Watanabe S, Kinoshita M, Horiguchi M, Nakamura T, Chonabayashi K, Hishizawa M, Hasegawa K, Kume N, Yokode M, Kita T, Kimura T, Ono K.

- MicroRNA-33 deficiency reduces the progression of atherosclerotic plaque in ApoE^{-/-} mice. *J Am Heart Assoc.* Dec.2012 1:e003376. [PubMed: 23316322]
38. Marquart TJ, Wu J, Luscis AJ, Baldan A. Anti-miR-33 Therapy Does Not Alter the Progression of Atherosclerosis in Low-Density Lipoprotein Receptor-Deficient Mice. *Arterioscl Throm Vas.* Mar. 2013 33:455–8.
39. Iqbal AJ, Regan-Komito D, Christou I, White GE, McNeill E, Kenyon A, Taylor L, Kapellos TS, Fisher EA, Channon KM, Greaves DR. A real time chemotaxis assay unveils unique migratory profiles amongst different primary murine macrophages. *PLoS One.* 8:e58744. [PubMed: 23516549]

Novelty and Significance

What Is Known?

- Compared to non-diabetics, diabetic patients have high rates of cardiovascular disease (CVD), low plasma levels of HDL, and attenuated risk reduction after plasma LDL-lowering therapies.
- Diabetic mice have impaired atherosclerotic plaque regression after plasma LDL lowering compared to non-diabetic mice, in part from monocytes associated with hyperglycemia.
- miR-33 controls HDL metabolism in mice and non-human primates through regulation of ABCA1, and is considered to be a potential anti-atherosclerosis therapeutic target.

What New Information Does This Article Contribute?

- After plasma LDL lowering, diabetic mice treated with anti-miR33 therapy had improved regression of atherosclerosis as indicated by decreases in the plaque content and inflammatory state of macrophages.
- Decreased plaque content of macrophages was explained by a reduction in hyperglycemia-associated monocytes as a result of anti-miR33 treatment and reduced recruitment of monocytes to plaques.
- Reduced monocytes reflected decreased proliferation of bone marrow monocyte precursors (BMP) most likely through upregulation of ABCA1, a factor known to regulate their proliferation.

The overwhelming cause of death in type 1 and 2 diabetic patients is CVD. Though diabetics have shown relative risk reduction in statin intervention trials, their absolute risk remains elevated, making the understanding of this phenomenon an important clinical need. Consistent with the clinical findings, in mouse models we showed that diabetes impairs atherosclerosis regression after aggressive lowering of high LDL levels. This impairment was traced to monocytes, which drives more monocytes into diabetic plaques. In pre-clinical studies by others, the cholesterol content of the monocyte BMP was positively associated with their proliferation. We now show, for the first time, that anti-miR-33 therapy reduced cellular cholesterol content by increasing ABCA1 in the diabetic monocyte BMP and decreased BMP proliferation. This prevented diabetic monocytes and decreased plaque recruitment of monocytes. We previously reported anti-inflammatory effects of anti-miR33 treatment on mouse plaque macrophages, and again observed these effects in diabetes. Thus, by reducing the content and inflammatory state of plaque macrophages after LDL lowering, anti-miR33 treatment was able to improve atherosclerosis regression in diabetic mice.

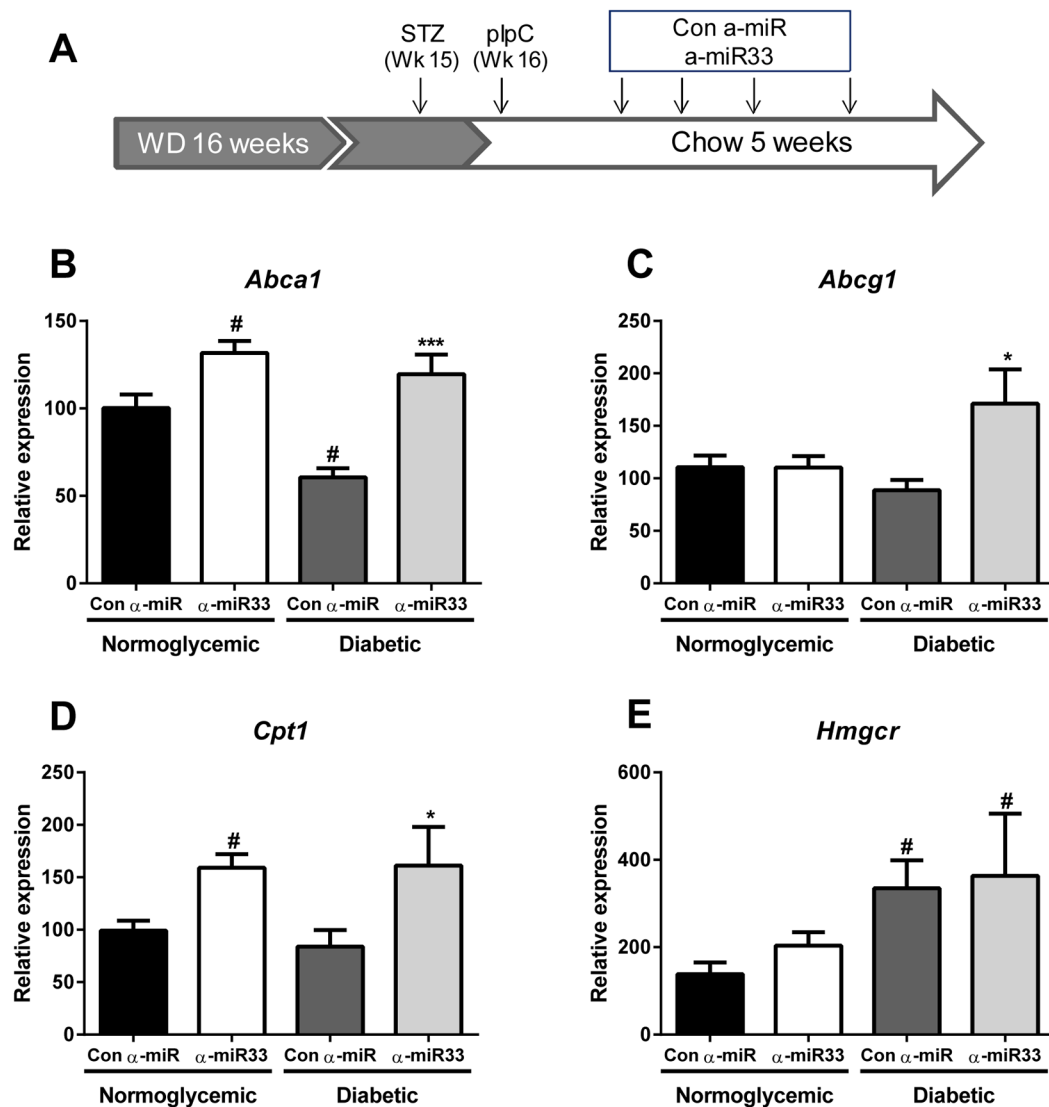


Figure 1. α -miR33 treatment derepresses its target genes in the liver of Reversa mice

(A) Experimental design: Reversa mice were placed on a western diet for 16 weeks. At 15 weeks, the mice received 5 injections of citrate (control) or 50mg/kg streptozotocin (diabetic). At 16 weeks, all mice were switched to a chow diet and received polyinosinic polycytidylic RNA (pIpC) 15 mg/kg every other day for a total of four injections to initiate lipid lowering. Mice then received weekly (s.c) injections of either control anti-miR or anti-miR33 2'F/MOE oligonucleotides (10mg/kg) for 4 weeks, prior to sacrifice (i.e 4 weeks post the final pIpC injection). Hepatic expression of (B) *Abca1*, (C) *Abcg1*, (D) *Cpt1* and (E) *Hmgcr*. # p 0.05 vs. con α -miR normoglycemic; * p 0.05, *** p 0.001 vs. con α -miR diabetic.

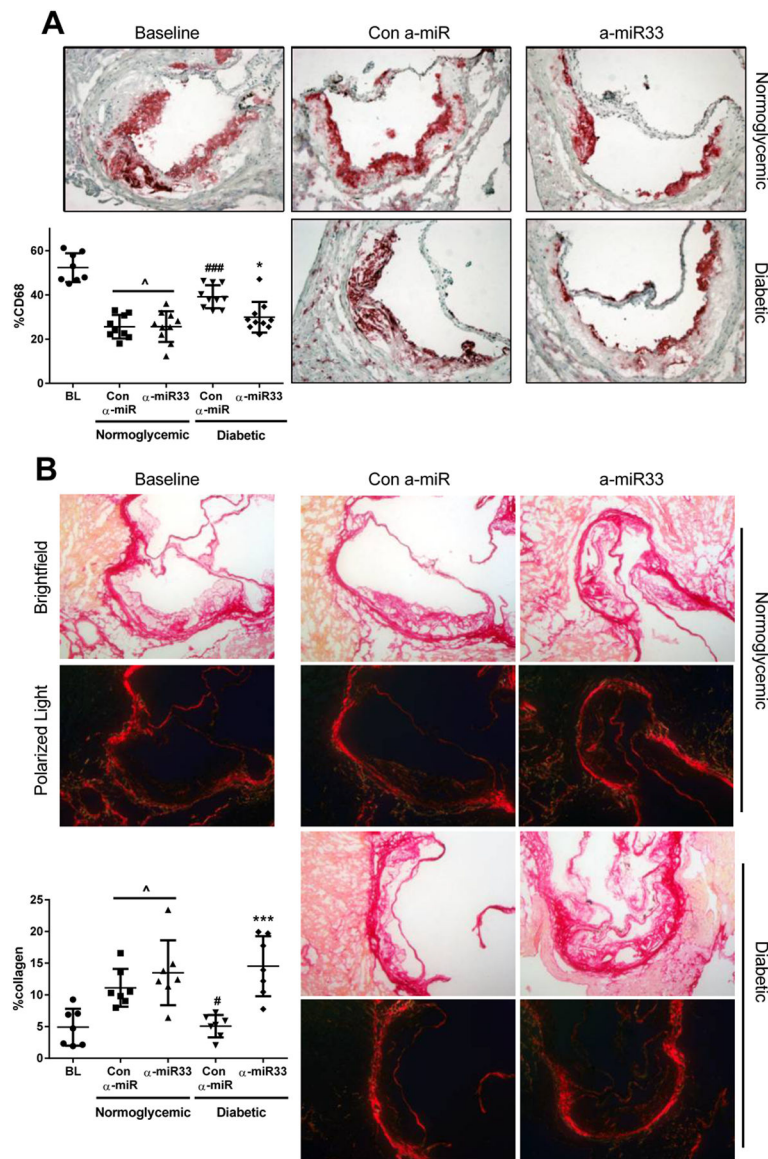


Figure 2. α -miR33 treatment restores regression in diabetic mice

Aortic roots from baseline and the regression groups were sectioned, fixed and stained for (A) CD68 and (B) collagen. Representative pictures of (A) CD68 immunostaining (magnification $\times 20$) and (B) picrosirius red staining (under white and polarized light) of collagen (magnification $\times 10$) are shown for each group. The areas of the plaques occupied by CD68+ cells and collagen (the latter as detected by polarized light) were quantified by Image Pro Plus Software and displayed in the graphs. Results are expressed as the percentage of plaque area. \wedge p 0.05 vs. baseline, # p 0.05, ### p 0.001 vs. con α -miR normoglycemic; *** p 0.001 vs. α -miR33 diabetic.

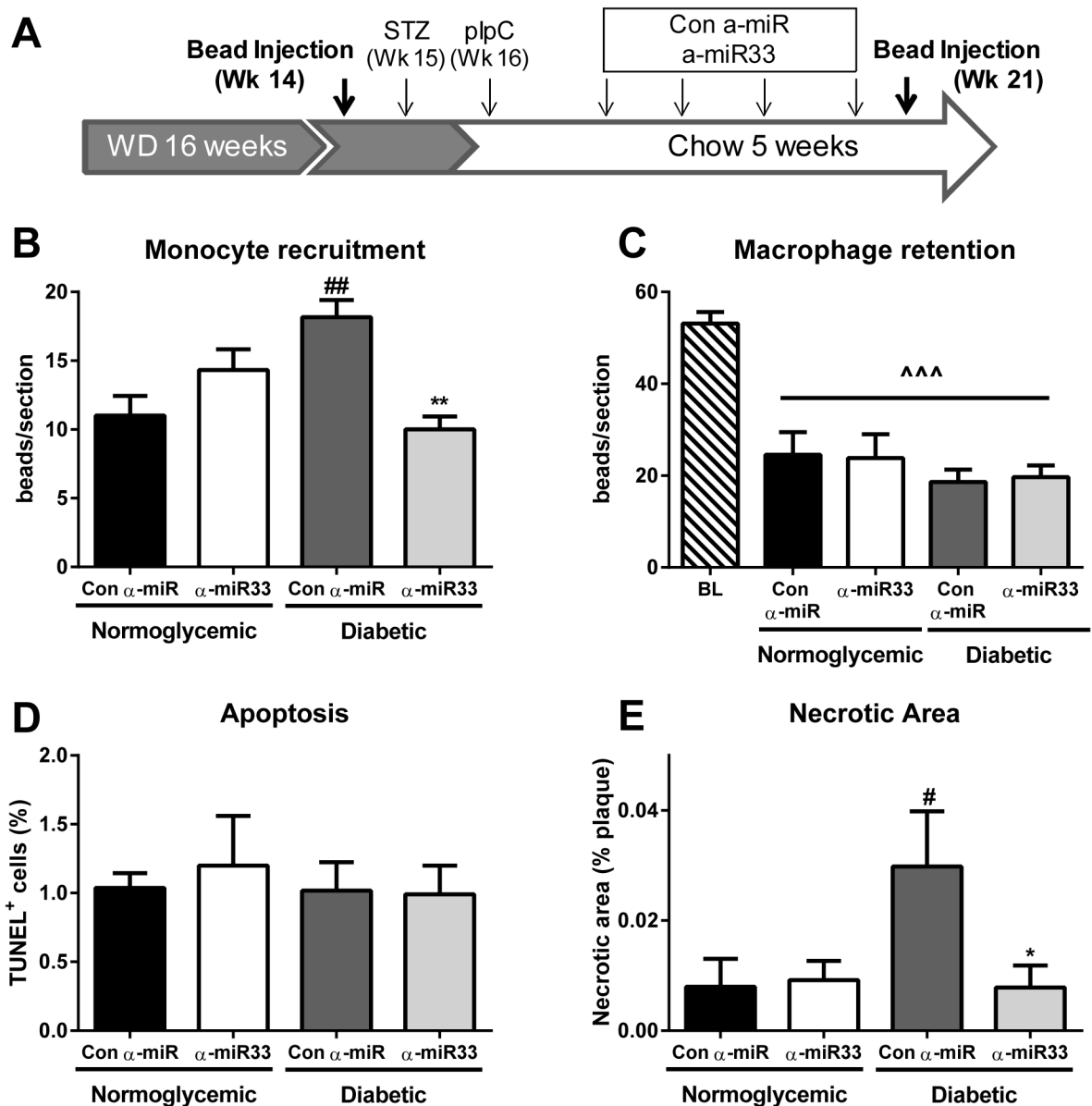


Figure 3. α-miR33 treatment affects monocyte trafficking to the plaque

Experimental design for monocyte trafficking. (A) Reversa mice were injected with fluorescent latex beads either 24h prior to harvesting (week 21) for the recruitment protocol or at week 14 of western diet for the egress protocol. (B) To assess monocyte recruitment mice were injected with fluorescent latex beads 24h prior to sacrifice, and beads counted in the aortic root. Data are expressed as mean ±SEM (n = 6 per group). ^{##} p < 0.01 vs. con α-miR normoglycemic ^{**} p < 0.01 vs. con α-miR diabetic. (C) To assess macrophage retention mice were injected with fluorescent latex beads at week 14, and the number of beads remaining at sacrifice used to assess macrophage retention (baseline was established 1 week post bead injection). Data are expressed as mean ±SEM (n = 6 per group). ^{^^} p < 0.001 vs. baseline. (D) Quantitative analysis of TUNEL⁺DAPI⁺ cells per section in the aortic root, after regression. Results are expressed as the percentage of total cells per plaque ±SEM (n=4 per group). (E)

Quantitative analysis of necrotic core area as a percentage of total plaque area \pm SEM (n = 6 per group) # p < 0.05 vs. con α -miR normoglycemic * p < 0.01 vs. con α -miR diabetic.

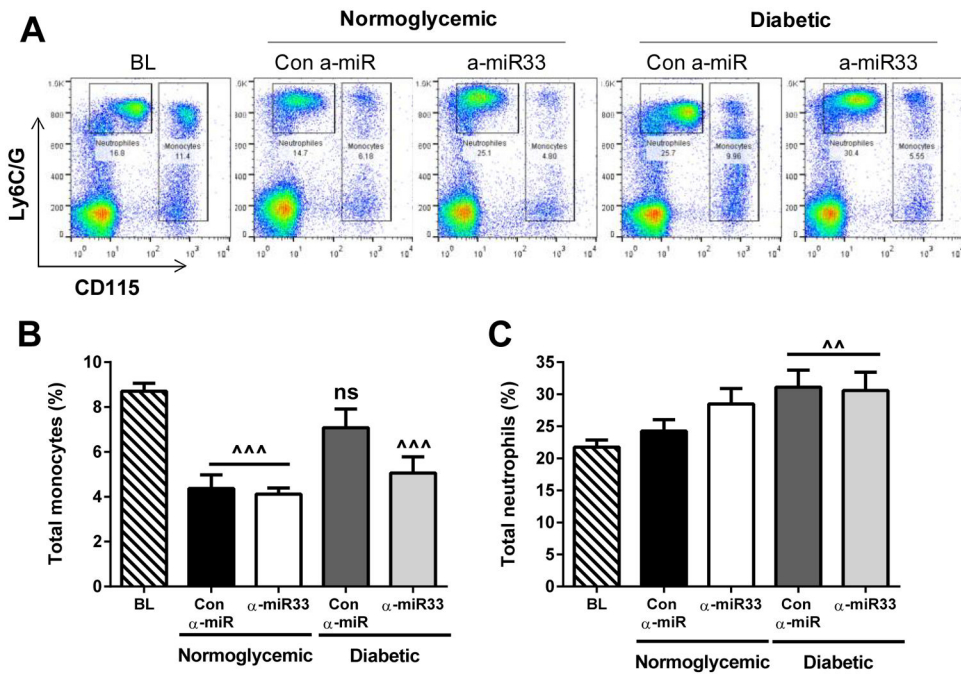


Figure 4. α -miR33 treatment decreases monocytosis in diabetic mice

Total monocytes and neutrophils were analyzed by flow cytometry in the blood at 16 weeks of diet (baseline) or after treatment. (A) Representative flow cytometry plots. Quantification of (B) monocytes and (C) neutrophils. Data are expressed as mean \pm SEM (n = 10 per group). ^^p 0.01, *** p 0.001 vs. baseline.

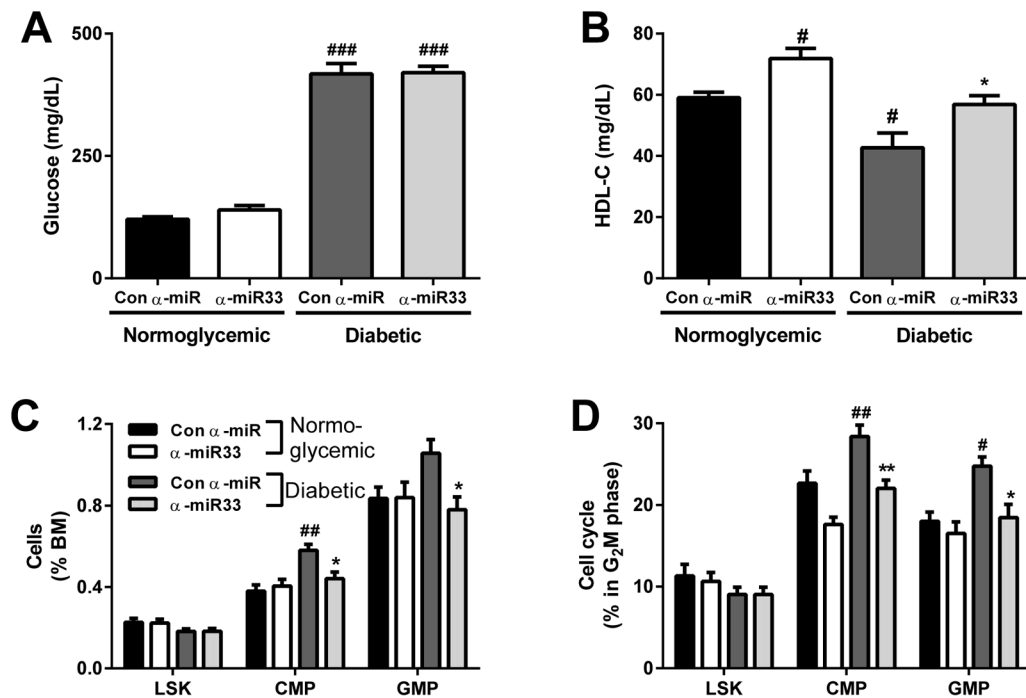


Figure 5. α -miR33 treatment decreases bone marrow progenitors in diabetic mice

C57Bl6/J mice were injected with citrate (normoglycemic) or 50mg/kg streptozotocin (diabetic). Mice were then injected 4 times with control α -miR or α -miR33 2'F/MOE oligonucleotides (10mg/kg). (A) Plasma blood glucose and (B) HDL-C 4 weeks post treatment. (C) Hematopoietic stem and progenitor cell populations in the BM were determined by flow cytometry and expressed as a percentage of cells in the BM. (D) Hematopoietic stem and progenitor cell cycle (G₂M phase) was assessed by flow cytometry using DAPI. Data are expressed as mean \pm SEM, n = 7/group. #p 0.05, ##p 0.01 vs. con α -miR normoglycemic; * p 0.05 con α -miR diabetic.

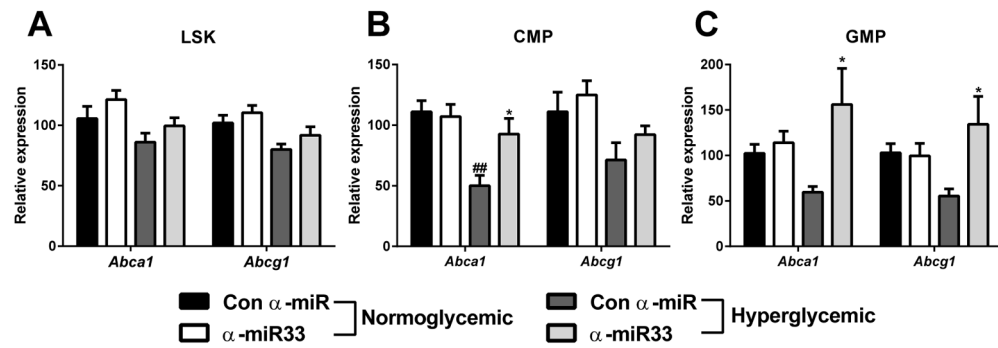


Figure 6. α -miR33 treatment restores *Abca1* expression in bone marrow progenitors of diabetic mice

C57Bl6/J mice were injected with citrate (normoglycemic) or 50mg/kg streptozotocin (diabetic). Mice were then injected 4 times with control α -miR or α -miR33 2'F/MOE oligonucleotides (10mg/kg). Gene expression for *Abca1* and *Abcg1* was assessed by qPCR in the different bone marrow progenitor subsets (A) LSK, (B) CMP and (C) GMP, obtained by cell sorting. Data are expressed as mean \pm SEM, n 7/group. #p 0.05, ##p 0.01 vs. con α -miR normoglycemic ;* p 0.05 vs. con α -miR diabetic.

Table 1
Plasma characteristics of Reversa mice after 5 weeks of α -miR control or α -miR33 treatment

Glycemia, total plasma cholesterol, HDL-C and triglyceride levels were obtained after 16 weeks of diet (baseline) and at sacrifice.

mg/dL	Baseline	Normoglycemic		Diabetic	
		Con α -miR	α -miR33	Con α -miR	α -miR33
Glucose	-	113±10	116±6	410±35 ^{****}	365±29 ^{****}
TC	863±46	101±14	93±10	83±13	94±9
HDL-C	35±3	25±3	33±3 [#]	35±2	50±6 [*]
TG	-	30±6	31±5	52±5 [#]	64±11 [#]

All data are expressed as mean \pm SEM (n>10).

[#] p 0.05 vs. con α -miR normoglycemic;

^{*} p 0.05,

^{****} p 0.001 vs. con α -miR diabetic.

Table 2

Gene expression analysis of laser-captured plaque CD68⁺ cells

CD68⁺ cells from aortic plaques of Reversa mice were isolated using LCM. mRNA was isolated, amplified and analyzed by RT-PCR. mRNA levels are presented as relative levels normalized to HPRT.

	Normoglycemic			Diabetic	
	Con	α -miR	α -miR33	Con α -miR	α -miR33
<i>α-miR33 targets</i>	<i>Abca1</i>	116±21	96±11	61±7 [#]	110±12 [*]
	<i>Abcg1</i>	115±25	111±15	146±19	116±20
<i>M2</i>	<i>Cd206</i>	129±44	223±70	108±23	192±49
	<i>Ym1</i>	252±115	2479±1588 [#]	92±30	527±170 [*]
<i>M1</i>	<i>Tnfa</i>	116±27	87±14	236±75	99±22
	<i>Il1β</i>	138±40	90±21	304±74 [#]	63±12 [*]
	<i>Nos2</i>	159±63	121±54	179±54	43±15
<i>Trafficking</i>	<i>Ccr2</i>	122±26	153±60	349±77 [#]	126±16 [*]
	<i>Ccr5</i>	124±27	119±13	154±26	120±27
	<i>Ccr7</i>	137±33	189±80	139±50	131±41
	<i>Netrin-1</i>	123±38	188±46	195±45	155±41
	<i>Unc5b</i>	113±23	139±25	121±19	117±32
<i>Adhesion</i>	<i>Vcam1</i>	103±12	138±27	2537±51 [#]	110±16 [*]
	<i>Icam1</i>	113±27	144±37	269±56	185±30

Data are expressed as mean ± SEM (n 6 per group).

[#] p 0.05 vs. con α -miR normoglycemic;

^{*} p 0.05 vs. con α -miR diabetic.